RESEARCH PAPERS

Acta Cryst. (1996). A**52**, 42–46

On the Anisotropy of Quasicrystal Structures

S. V. DIVINSKI* AND V. N. DNIEPRENKO

Institute of Metal Physics, Ukrainian Academy of Sciences, Vernadskogo 36, Kiev 142, 252680 Ukraine. E-mail: divin@d24imp.kiev.ua

(Received 9 February 1995, accepted 29 June 1995)

Abstract

Textures of melt-spun icosahedral and decagonal quasicrystals have been analysed *via* texture simulation by a sum of limited fibre components. The model has been extended to include the axial textures with an anisotropic spread of the texture axis. An orientation distribution function of the textured icosahedral quasicrystal has been calculated. It is shown that textured decagonal structures may exhibit an anisotropy of physical properties even in the ribbon plane.

1. Introduction

Alloys with quasiperiodic structures and rotational symmetries 'forbidden' by conventional crystallography have attracted much attention because of their unusual properties. Shechtman, Blech, Gratias & Cahn (1984) first observed such phases and detected 5-fold rotational symmetry. Later, quasicrystals with 8-fold, 10-fold and 12-fold axes were discovered; for a review, see Kelton (1994).

Melt spinning is known to be a method of quasicrystal fabrication. In the case of conventional crystals, such a solidification technique gives rise to crystallographic texture formation through preferred growth and/or nucleation (Chang, Bye, Laxmanan & Das, 1984; Arai, Tsutsumitake & Ohmori, 1984). Melt-spun quasicrystals also turn out to have a texture (Ino, Edagawa, Kimura, Takeuchi & Nasu, 1987; Sugawara, Edagawa, Oda, Seki, Ito, Ino, Kimura & Takeuchi, 1989; Edagawa, Sugawara, Oda, Seki, Ito, Ino, Kimura & Takeuchi, 1991). The texture can change the anisotropy of the physical properties and, therefore, must be taken into account.

To determine the anisotropy of the physical properties of textured phases, the function of the distribution of structure elements on orientations [orientation distribution function (ODF)] must be known (Bunge, 1987). The ODF is usually reproduced by numerical techniques from diffraction data of the pole-figure type. This method is not derived for quasicrystal symmetries yet. Moreover, it is known (Bunge, 1987) that, if the orientation symmetry is higher, the ghost effects of numerical ODF reproduction must be more pronounced. For example, while we may calculate half of the series-expansion coefficients for cubic crystalline symmetry (only even coefficients), only 30% of the coefficients may be obtained for hexagonal crystals (Bunge, 1987).

The ghost phenomena of ODF reproduction may be by-passed by the direct ODF approximation in an analytical form. This paper deals with the investigation and simulation of textures (both pole figures and ODFs) of the quasicrystal phases with icosahedral and decagonal symmetries.

2. Description of crystallographic textures

To approximate real textures in an analytical form, a number of approaches have been developed (Bunge, 1987; Matthies, 1982; Savelova, 1984; Dnieprenko & Divinski, 1992; Eschner, 1992; Nikolaev, Savelova & Feldmann, 1992). These models differ both in the form of their analytic presentations and in their approach to texture description.

In the present work, the textures of melt-spun quasicrystals are analysed. In such a case, both axial textures and textures with a dispersion concentrated around preferred orientations may arise in crystalline ribbons, with the axial textures being the most frequently observed (Arai, Tsutsumitake & Ohmori, 1984). The presence of some directions or texture axes, which allow the texture dispersion to be described by rotations around these axes, is a common feature of all these textures. This is dictated by specific crystallization conditions primarily by the direction of the temperature gradient and the conditions of nucleation and growth. Note that these characteristic directions may not coincide with the direction of the normal to the ribbon plane. In the very exceptional case of isotropic dispersion around preferred orientations (the so-called spherical components), one may resort to the model of Bunge (1987) or Matthies (1982) to describe analytically these textures.

However, both axial textures and textures intermediate between axial and spherical have been observed in melt-spun quasicrystals. All these textures are markedly anisotropic with the characteristic axis of the dispersion formation. In this case, the approach based on texture

©1996 International Union of Crystallography
Printed in Great Britain – all rights reserved

description by a superposition of limited fibre components is likely to be the most applicable (Dnieprenko & Divinski, 1992, 1993, 1994). It is noteworthy that all other techniques by which the anisotropic texture dispersions may be approximated (Savelova, 1984; Eschner, 1992; Nikolaev *et al.*, 1992) do not use the above-mentioned presentations about the texture axes.

The main feature of our approach is that the spread of each texture component must be described in its own local coordinate system. These systems are strongly connected with the texture axes introduced above for each component (in general, the texture may consist of a number of different components). In this work, however, all the following considerations will be carried out for a single-component texture to simplify the mathematical treatment. Generalization to the case of multicomponent textures is obvious. For most real textures, the position of the texture axes can be readily determined by experiment (Dnieprenko & Divinski, 1992) and textures of quasicrystals are among them. The best choice of a zero approximation for its position is an orientation of the highest maximum in the pole figures and the precise position can be found by a subsequent iteration procedure (Dnieprenko & Divinski, 1993).

Thus, we will describe the ODF f of a quasicrystal structure in the local coordinate system by the following expression:

$$f(g_\gamma) = A\exp\{-\gamma_2^2/2\sigma_1^2\}\exp\{-\tfrac{1}{2}[(|\gamma_1+\gamma_3| - \sigma_3 + |\sigma_3 - |\gamma_1+\gamma_3||)/2\sigma_2]^2\}. \quad (1)$$

The Eulerian angles $g_\gamma = (\gamma_1, \gamma_2, \gamma_3)$ define the grain orientation with respect to the local coordinate system introduced above; $\sigma_1, \sigma_2, \sigma_3$ are the spread parameters. The σ_3 value determines the length of the regions in the g_γ orientation space with a constant orientation density. Now we must take into account the position of the local coordinate system (or the texture axis) with respect to the external directions. Thus, grain orientation $g_B(\varphi_1, \Phi, \varphi_2)$ in the external coordinate system of a sample may be obtained *via* the angles $\gamma_1, \gamma_2, \gamma_3$ by

$$g_B = g_0 g_\gamma g_1 = g_0 g_\gamma [g_0]^{-1} g_B^0, \quad (2)$$

where $g_0(\Psi_0, \theta_0, \varphi_0)$ specifies the transformation to the local coordinate system and $g_1(\Psi_1, \theta_1, \varphi_1)$ does a back-transformation to the $\varphi_1, \Phi, \varphi_2$ angles. In (2), we take into account that the g_γ matrix is a unit one if the $\gamma_1, \gamma_2, \gamma_3$ angles equal zero, and all the rotations g_0, g_1 must determine the preferred orientation g_B^0.

The ODF $f(g_B)$ must satisfy symmetry relations of the following type: $f(g_B) = f(g_B^q \cdot g_B \cdot g_B^s)$, where g_B^q and g_B^s are the elements of the point groups G^q and G^s and they describe the symmetry transformations of the quasicrystal and the sample, respectively. Taking this into account, we find that the 'elementary cell' in the orientation space $g_B = (\varphi_1, \Phi, \varphi_2)$ will be $0 \le \varphi_1 \le \pi/2$, $0 \le \Phi \le \pi/2$, $0 \le \varphi_2 \le 2\pi/5$ for the icosahedral quasicrystal symmetry and the orthotropic texture symmetry.

To allow for the symmetry relations, we have to take into account that there are M crystallographically identical orientations of the preferred maximum. Thus, we have

$$f_B(\varphi_1, \Phi, \varphi_2) = \sum_{l=1}^{M} f(\gamma_1^{(l)}, \gamma_2^{(l)}, \gamma_3^{(l)}), \quad (3)$$

where $\gamma_1^{(l)}, \gamma_2^{(l)}, \gamma_3^{(l)}$ are determined by

$$g_\gamma^{(l)} = [g_0^{(l)}]^{-1} g_B [g_B^0]^{-1} g_0^{(l)}. \quad (4)$$

Here, l is an index that numbers consecutively these crystallographically identical orientations.

3. Pole figures

The pole density $P_{\{\bar{\mathbf{H}}\}}(\bar{\mathbf{y}})$ of the pole figure $\{\bar{\mathbf{H}}\}$ can be calculated as follows:

$$P_{\{\bar{\mathbf{H}}\}}(\bar{\mathbf{y}}) = \sum_{i=1}^{M} (2\pi M)^{-1} \int_0^{2\pi} f(\gamma_1^{(i)}, \gamma_2^{(i)}, \gamma_3^{(i)})\,\mathrm{d}\delta, \quad (5)$$

where $g_\gamma^{(i)} = g_0^{-1} g_B^{(i)} \Omega(\delta) [g_B^0]^{-1} g_0$; $g_B^{(i)}$ is the matrix of rotations and is determined by the condition $\bar{\mathbf{y}} = \bar{\mathbf{h}}_i g_B^{(i)}$, where $\bar{\mathbf{h}}_i, i = 1, \ldots, M$, are equivalent planes from the $\{\bar{\mathbf{H}}\}$ family; $\Omega(\delta)$ is the matrix of rotation by the δ angle around $\mathbf{y}$. The rest of the designations are the same as in (3) and (4).

4. Textures of melt spinning

Let us consider the texture types that are most often formed in the process of rapid solidification.

The texture of the icosahedral phase in melt-spun $Al_{72}Si_6Fe_{5.5}Mn_{16.5}$ may be described as an axial texture with a spherical dispersion of the texture axis (Ino *et al.*, 1987). The texture of *i*-$Al_{60}Li_{30}Cu_{10}$ exhibits dispersion close to the axial one but with a pronounced anisotropy of the spread of the texture axis with respect to the normal to the ribbon plane (Sugawara *et al.*, 1989). In this case, the angular spread of the texture axis in the ribbon direction is markedly smaller than that along the transversal direction.

Moreover, we found that a similar texture is formed in melt-spun *i*-$Al_{86}Fe_{14}$, see Fig. 1. Here, however, the texture-axis dispersion is less anisotropic and is intermediate between the above-mentioned two limiting texture types. In all these cases, the normal to the ribbon plane serves as a crystallization axis and coincides with the 5-fold crystallographic direction [100000]. The same orientation of growth direction has been found in *i*-AlLiCu (Gaybe, 1987) and in *i*-TiFeMnSi (Zhang & Kelton, 1992). Nevertheless, it has been reported in a number of studies that growth from the liquid may be most rapid along the threefold direction (Shaefer,

Bendersky, Shechtman, Boettinger & Biancaniello, 1986; Nissen, Wesichen, Beeli & Gsanady, 1988). Thus, the crystalloraphic orientation of the growth direction is likely to depend on particular nucleation and growth conditions.

We also investigated the direction of preferred crystallization in decagonal quasicrystals under rapid solidification. In d-$Al_{62}Cu_{20}Co_{15}Si_3$ ribbon, we observed an axial texture with a marked anisotropy of dispersion of the texture axis, see Fig. 2. The 10-fold axis is the texture axis in this case and it is deflected from the normal to the ribbon plane by a small angle of about 5°.

Axial textures with virtually spherical dispersion are very simple and can be approximated by (1) at $\sigma_2 = \infty$ and an arbitrary value of σ_3. When there is some deflection of the texture axis from the normal position, the analytic form of (1) remains the same since it refers to the local coordinate system of the texture axis. Only values of rotations g_1 that transform the texture dispersion previously formed to the final position will change. By such means, the pole figures of i-$Al_{86}Fe_{14}$ (Fig. 1) can be directly simulated both in our approach and with Bunge-type model functions.

However, to simulate the quasicrystal textures, the anisotropic spread of the texture-axis position relative to the sample coordinate system must be introduced (from angles g_B^0, *i.e.* by the position of the preferred orientation in this coordinate system). Also, the crystallographic position of the texture axis must be unchanged, *i.e.* g_0 remains constant in (2) and (4). To include the anisotropic spread of the texture axis, we write

$$f_B(\varphi_1, \Phi, \varphi_2) = M^{-1} \sum_{l=1}^{M} \int_{g'_B} F(g'_B) f(\gamma_1^{(l)}, \gamma_2^{(l)}, \gamma_3^{(l)})\, \mathrm{d}g'_B \qquad (6)$$

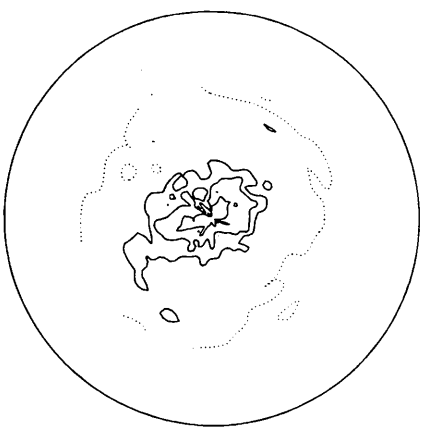

{100000}
(*a*)

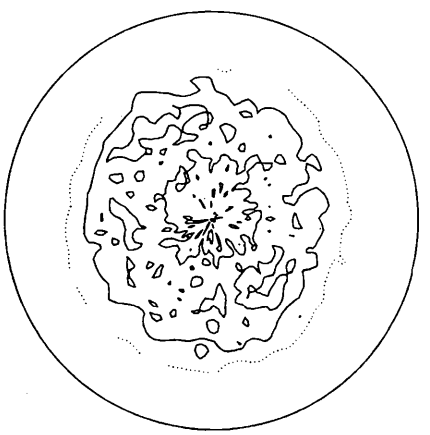

{110000}
(*b*)

Fig. 1. Pole figures of i-$Al_{82}Fe_{18}$. Intensity levels are (in counts): (*a*) 1000, 1200, 1300, 1450 and (*b*) 700, 850, 950. The lowest level is shown as a dotted curve.

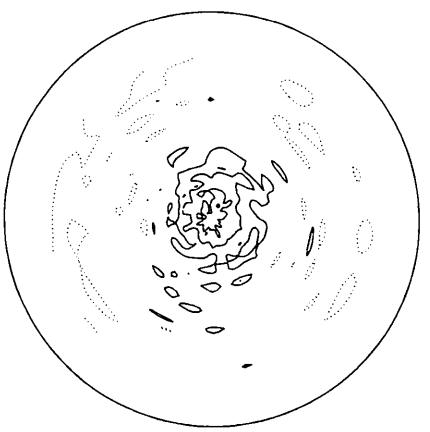

{100000}
(*a*)

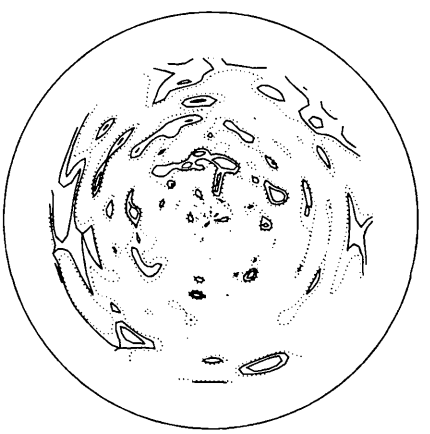

{110000}
(*b*)

Fig. 2. Pole figures of d-$Al_{62}Cu_{20}Co_{15}Si_3$. Intensity levels are (in counts): (*a*) 1430, 1600, 1700, 1860 and (*b*) 1450, 1470, 1500. The lowest level is shown as a dotted curve.

instead of (3). The matrix $g_\gamma^{(l)} = g_\gamma^{(l)}(\gamma_1^{(l)}, \gamma_2^{(l)}, \gamma_3^{(l)})$ is determined by $g_\gamma^{(l)} = [g_0^{(l)}]^{-1} g_B [g_B']^{-1} g_0^{(l)}$ depending on the current position of the texture axis g_B' in the external coordinate system. The $F(g_B')$ function describes the spread of the texture-axis position and is defined by the general approach of (1)–(4):

$$F(g_B') = f(\gamma_1', \gamma_2', \gamma_3'), \quad g_\gamma' = [g_0']^{-1} g_B' [g_B'^0]^{-1} g_0'. \tag{7}$$

Here, $f(\gamma')$ is a function of type (1), and g_0' and $g_B'^0$ have the same sense as the corresponding matrices in (2).

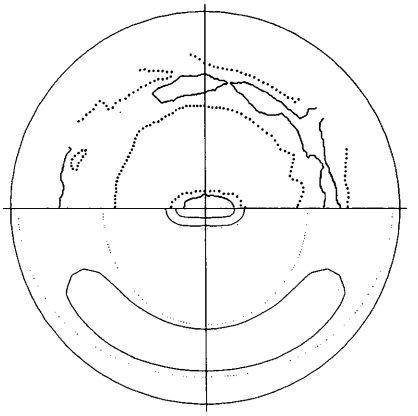

{100000}

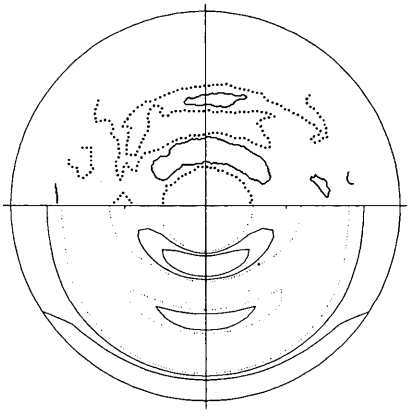

{110000}

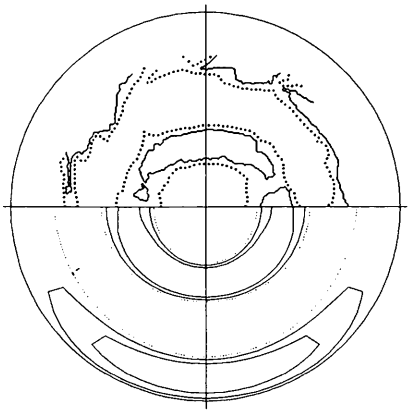

{110001}

Fig. 3. Comparison of model pole figures (bottom) and experimental ones for i-$Al_{60}Li_{30}Cu_{10}$ (Edagawa *et al.*, 1991) (top) for axial texture with an anisotropic spread of the texture axis.

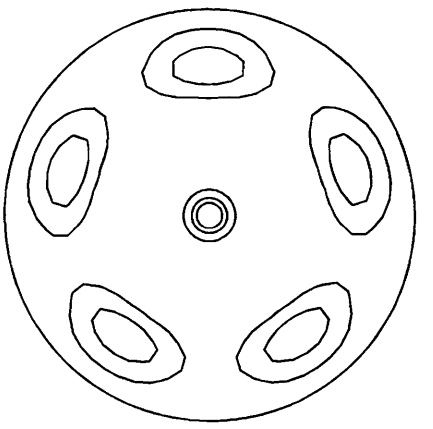

{100000}

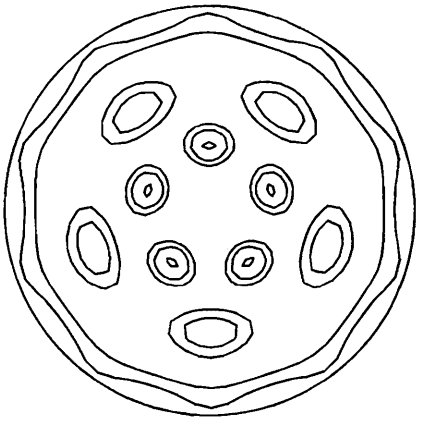

{110000}

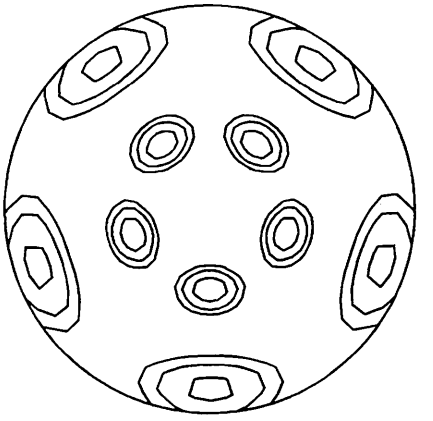

{110001}

Fig. 4. Hypothetical model pole figures for a case of limited fibre texture, $\sigma_1 = 8$, $\sigma_2 = 16$ and $\sigma_3 = 0°$.

Now, (6) and (7) allow the axial textures to be simulated with an anisotropic spread of texture axes that is experimentally observed in the melt-spun quasicrystals. The axial textures were simulated by setting $\sigma_2 = \infty$. In this case, the σ_3 value has no sense and may be chosen as arbitrary. In Fig. 3, the {100000}, {110000} and {110001} model pole figures along with the experimental pole figures for i-$Al_{60}Li_{30}Cu_{10}$ (Edagawa *et al.*, 1991), which form the basis for the numerical approximation, are presented. Fitted values of model parameters are $\sigma_1 = 7°$ and $\sigma_2 = \infty$. The model is seen to agree well with the experimental data. Heterogeneity of the pole density dispersion with respect to the axis observed in the {110000} and {110001} pole figures can be directly explained by the texture simulation, that is by the presence of the anisotropic dispersion of the texture axis.

Strict axial symmetry of dispersion with respect to the texture axis may be violated and, thus, we must account for $\sigma_2 \neq \infty$ in (1). For example, a tendency towards the appearance of limited fibre textures may be traced in pole figures of i-$Al_{68}Si_4Ru_8Mn_{20}$ (Sugawara *et al.*, 1989). To simulate such a texture type, we choose the following parameters: $\sigma_1 = 8, \sigma_2 = 16$ and $\sigma_3 = 0°$. Model pole figures {100000}, {110000}, {110001} and corresponding ODF are shown in Figs. 4 and 5, respectively. It is seen that the separate maxima in the pole figures are substantially overlapped owing to a high symmetry of the quasicrystals. In this case, the use of the ODF approach allows separate components to be identified with a higher degree of reliability.

For the quasicrystal phases with an n-fold symmetry axis ($n = 8, 10$ and 12), the elementary cell in the ODF space transforms to $0 \leq \varphi_1 \leq \pi/2$, $0 \leq \Phi \leq \pi/2$, $0 \leq \varphi_2 \leq 2\pi/n$. In this case, the ODF analysis may be carried out as in (1)–(3).

Heretofore, textures of melt-spun quasicrystals have been considered. We found that the decagonal phase in the $Al_{62}Cu_{20}Co_{15}Si_3$ alloy produced by the conventional slow casting technique does not exhibit any texture. Nevertheless, is should be noted that the present analysis with an obvious correction of the ODF parameters can be fully applied to textures that may accompany an arbitrary technical process of the quasicrystal fabrication.

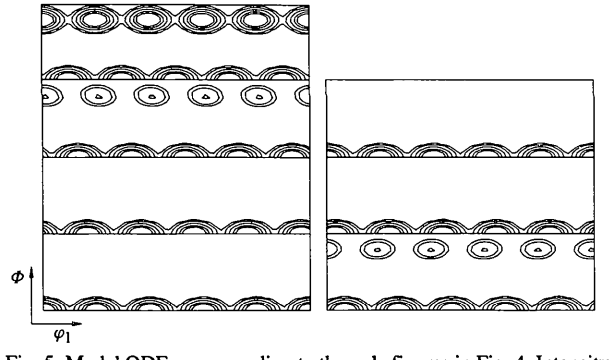

Fig. 5. Model ODF corresponding to the pole figures in Fig. 4. Intensity levels are: 1, 2, 5, 10, 15 in random distribution units.

In conclusion, we note that this model of quasicrystal textures may serve as a 'touchstone' for numerical techniques of the ODF reproduction by diffraction data to exclude the ghost effects. Moreover, our approach to the analytical ODF description may be used to allow for texture contribution to anisotropy of physical properties of the quasicrystal materials, especially for the decagonal phases. Averaging of tensor values over the texture can be carried out similar to Divinski & Dnieprenko (1994). Asymmetry of texture-axis dispersion may play a crucial role in accurate anisotropy calculation and may result in a marked anisotropy of physical properties of decagonal quasicrystals even in the ribbon plane.

This study was supported by the Ukrainian State Science and Technology Committee under grant no 4.3/56.

References

Arai, K.-I., Tsutsumitake, H. & Ohmori, K. (1984). *J. Jpn. Inst. Met.* **48**, 482–488.

Bunge, H. J. (1987). Editor. *Theoretical Methods of Texture Analysis*. Oberursel: DGM Informationsgesellschaft.

Chang, C. F., Bye, R. L., Laxmanan, V. & Das, S. K. (1984). *IEEE Trans. Magn.* **20**, 553–558.

Divinski, S. V. & Dnieprenko, V. N. (1994). *J. Phys. Condens. Matter*, **6**, 8503–8512.

Dnieprenko, V. N. & Divinski, S. V. (1992). *Scr. Metall.* **27**, 1617–1622.

Dnieprenko, V. N. & Divinski, S. V. (1993). *Textures Microstruct.* **22**, 73–85.

Dnieprenko, V. N. & Divinski, S. V. (1994). *Textures Microstruct.* **22**, 169–175.

Edagawa, K., Sugawara, T., Oda, K., Seki, F., Ito, K., Ino, H., Kimura, K. & Takeuchi, S. (1991). *J. Jpn. Inst. Met.* **56**, 607–614.

Eschner, T. (1992). *Textures Microstruct.* **20**, 139–146.

Gaybe, F. W. (1987). *J. Mater. Res.* **2**, 1–13.

Ino, H., Edagawa, K., Kimura, K., Takeuchi, S. & Nasu, S. (1987). *Mater. Sci. Forum*, **22–24**, 437–452.

Kelton, K. F. (1994). *Intermetallic Compounds*, edited by J. H. Westbrook & R. L. Fleischer, Vol. 1, pp. 453–491. New York: John Wiley.

Matthies, S. (1982). *Phys. Status Solidi B*, **112**, 705–716.

Nikolaev, D. I., Savelova, T. I. & Feldmann, K. (1992). *Textures Microstruct.* **19**, 9–27.

Nissen, A. U., Wesichen, M., Beeli, G. & Gsanady, A. (1988). *Philos. Mag.* **B57**, 587–598.

Savelova, T. I. (1984). *Zavod. Lab.* **50**, 48–52. (In Russian.)

Shaefer, R. J., Bendersky, L. A., Shechtman, D., Boettinger, W. J. & Biancaniello, F. S. (1986). *Metall. Trans.* **17A**, 2117–2125.

Shechman, D., Blech, I., Gratias, D. & Cahn, J. W. (1984). *Phys. Rev. Lett.* **53**, 1951–1953.

Sugawara, T., Edagawa, K., Oda, K., Seki, F., Ito, K., Ino, H., Kimura, K. & Takeuchi, S. (1989). *Scr. Metall.* **23**, 711–716.

Zhang, X. & Kelton, K. F. (1992). *Scr. Metall. Mater.* **26**, 393–398.